We sincerely thank this reviewer for the valuable comments. Our detailed responses and corresponding revisions are provided below. The final revised manuscript will incorporate these and the comments from other reviewers.

Introduction:

1.

Comment: Line 59, the reference to Mariethoz et al. 2010 (Direct Samling specific algorithm, as mentioned line 551) might not be the most appropriate to support your statement here. Guardiano and Srivastava 1993 instead?

Reply to the reviewer: We recognize that MPS was first proposed by Guardiano and Srivastava (1993) and the reference was added. However, we also think it is important to propose a more recent reference for MPS, to guide the readers towards successful applications.

Original: '*Multiple-Point Statistics (MPS) has become a widely used geostatistical method in hydrostratigraphical modelling. MPS uses Training Images (TIs) to quantify the spatial variability and reproduce complex geological patterns that cannot be captured by traditional two-point geostatistics (Mariethoz et al. 2010)*'

Revision:'*Multiple-Point Statistics (MPS) has become a widely used geostatistical method in hydrostratigraphical modelling. MPS uses Training Images (TIs) to quantify the spatial variability and reproduce complex geological patterns that cannot be captured by traditional two-point geostatistics (Guardiano and Srivastava, 1993; Mariethoz and Caers, 2014)*'

2.

Comment: Line 69: what do you mean by that? How does the reference to Meerschman et al. 2013 support this statement? This reference would better describe the ease of use or wide use of MPS techniques such as the Direct Sampling.

Reply to the reviewer: It is right that Meerschman et al. (2013) did not treat specifically the case of geophysics. The sentence was revised, and a reference to Lochbühler et al. (2014) was added to support the statement.

Original: '*Moreover, the integration of geophysical data is often heuristic and lacks a formally probabilistic structure (Meerschman et al., 2013).*'

Revision:'*Most existing MPS approaches, such as Direct Sampling (Meerschman et al., 2013), still treat soft or geophysical data in a heuristic manner, through secondary training images rather than probabilistic conditioning (e.g., Lochbühler et al., 2014), so they cannot explicitly address vertical non-stationarity within a probabilistic framework.*'

3.

Comment: Many statements refer to 4 different citations. Maybe keep the two most relevants and cite as (e.g. …).

Reply to the reviewer: Thanks for noticing this. We modified the text accordingly.

Original: '*Incorporating uncertainty into the simulation of geological heterogeneity, geostatistical approaches provide not only plausible geological scenarios but also essential input for ensemble-based hydrogeological forecasting, which is one type of probabilistic approach that relies on multiple realizations to assess model uncertainty. (Moore et al., 2022; Zimmerman et al., 1998; Enemark et al., 2024; Hermans et al., 2015).*'

Revision: '*Incorporating uncertainty into the simulation of geological heterogeneity, geostatistical approaches provide not only plausible geological scenarios but also essential input for ensemble-based hydrogeological forecasting, which is one type of probabilistic approach that relies on multiple realizations to assess model uncertainty. (e.g. Enemark et al., 2024; Hermans et al., 2015).*'

4.

Comment: Relevant work that could probably be included in the literature review:
Lochbühler, T., Pirot, G., Straubhaar, J., & Linde, N. (2014). Conditioning of multiple-point statistics facies simulations to tomographic images. Mathematical Geosciences, 46(5), 625-645.
Pirot, G., Linde, N., Mariethoz, G., & Bradford, J. H. (2017). Probabilistic inversion with graph cuts: Application to the Boise Hydrogeophysical Research Site. Water Resources Research, 53(2), 1231-1250.

Original: '*Madsen et al. (2021) proposed treating uncertain geological interpretations as probabilistic constraints, comparing MPS and Gaussian simulation methods, and showed that MPS produced more geologically plausible and connected realizations. Hermans et al. (2015) developed a full MPS-based inversion framework that used ERT data both to falsify prior geological scenarios and to locally constrain groundwater simulations, showing the strength of MPS in quantifying uncertainty and integrating multiple data types.*'

'*Although geophysical data do not directly measure lithology, they provide property contrasts (e.g., in resistivity) that, after inversion and interpretation, can be statistically linked to hydrofacies distributions (Michel et al., 2020; Looms et al., 2008).*'

Revision: '*Madsen et al. (2021) proposed treating uncertain geological interpretations as probabilistic constraints, comparing MPS and Gaussian simulation methods, and showed that MPS produced more geologically plausible and connected realizations. Hermans et al. (2015) developed a full MPS-based inversion framework that used ERT data both to falsify prior geological scenarios* *and to locally constrain groundwater simulations, showing the strength of MPS in quantifying uncertainty and integrating multiple data types. Lochbühler et al. (2014) demonstrated that tomographic images can be used to condition multiple-point statistics facies simulations, thereby improving the structural consistency of simulated geological models.*'

'*Although geophysical data do not directly measure lithology, they provide property contrasts (e.g., in resistivity) that, after inversion and interpretation, can be statistically linked to hydrofacies distributions (Michel et al., 2020; Pirot et al. 2017).*'

5.

Comment: You have to clarify in the introduction that you are building up on previous work (Isunza Manrique et al., 2023) or ideas presented at a conference (Guo et al. 2024) and explain what is new here.

Reply to the reviewer: A preliminary version of this study was presented by us at a conference (Guo et al., 2024), where the integration of geophysical inversion with the MCP framework was demonstrated using a synthetic case. The present manuscript extends this framework to a real-world 3D geological setting and includes detailed quantitative assessments of uncertainty reduction and model sensitivity. Although the principle of permanence of ratios has also been applied by Isunza Manrique et al. (2023) to combine probabilistic information from multiple geophysical attributes, specifically resistivity and chargeability, their approach focuses on probabilistic interpretation of inversion results and does not include geostatistical simulations. In contrast, the present study extends the work of Benoit et al. who developed the MCP framework and use the permanence of ratio to formally integrate probabilistic geophysical information into the MCP realizations.

Original： '*A recently applied geostatistical approach by Benoit et al. (2018), known as Markov-type Categorical Prediction (MCP), provides an alternative framework to traditional multiple-point statistics (MPS) for simulating categorical geological units. MCP uses bivariate transition probabilities derived from a training image. One of the key advantages of MCP is that it reduces the dependence on high-quality or highly repetitive training images, which can be a limiting factor in some MPS implementations (Allard et al., 2011).. When key features in the TI are sparse, irregular, or unique, MPS may struggle to reproduce them consistently, potentially leading to artificial discontinuities or oversimplified realizations (Barfod et al., 2018). By contrast, MCP operates on a different principle. Rather than trying to reproduce entire patterns from the TI, MCP uses pairwise transition probabilities between units to capture the likelihood of one unit being adjacent to another (Benoit et al., 2018). This approach allows MCP to extract essential geological information in a non-stationary fashion without needing a complete TI. Furthermore, MCP remains computationally efficient, even when simulating models with a large number of lithological categories because it avoids high-order pattern scanning or search-tree construction. One of MCP's strengths is its ability to strictly respect geological rules when certain transitions between units are geologically impossible. For example, if a specific lithological unit is never observed directly above another in the training data, MCP ensures that this configuration will not appear in the simulated model based* *on zero bivariate probability of these two units (Benoit et al., 2018). Yet, previous applications of the MCP framework have relied almost exclusively on hard conditioning data, such as borehole lithology. In settings where such data are sparse, the method often defaults to random simulation, which can result in geologically unrealistic outputs (Benoit et al., 2018). However, MCP offers greater transparency and flexibility in conditioning, making it well suited for the integration of soft information derived from geophysical inversion models. To leverage this potential, our study extends the MCP framework by incorporating geophysical soft constraints into the simulation process. This integration aims to reduce uncertainty and enhance the geological realism of subsurface models, particularly in areas that are poorly constrained by hard data.*'

Revision: Insert the following paragraph after the one above: '*A preliminary version of this work was presented at a conference (Guo et al., 2024), where the feasibility of integrating geo-physical inversion results into the MCP framework was demonstrated using a synthetic case. Building on that foundation, the present study extends the approach to a real-world 3D geological setting and includes a comprehensive quantitative evaluation of uncertainty reduction and model sensitivity. In this work, soft information derived from geophysical inversion models is merged into the MCP framework using the principle of permanence of ratios from the study of Isunza Manrique et al. (2023), where they combined probabilistic information from multiple geophysical attributes such as resistivity and chargeability. However, their work was limited to the probabilistic interpretation of inversion results without performing geostatistical simulations. In contrast, our study integrates this principle directly within the MCP simulation process, enabling the formal incorporation of probabilistic geophysical information into the categorical realization generation. This represents a methodological advancement over existing MCP applications by linking geostatistical simulation with geophysically derived probability fields, thereby improving both geological realism and interpretability of subsurface models.*'

Method：

6.
Comment: 2.1 MCP: Is the considered lag h omnidirectional or directional?

Reply to the reviewer: In the MCP algorithm, the lag h=(hx, hy, hz) represents directional lag vector between the simulated node and its neighboring nodes. For each pair of facies categories (i,j), the precomputed matrix $gh_{ij}(hx, hy, hz)$ stores the bivariate probabilities as a function of this lag. During simulation, for each node, the algorithm retrieves the corresponding probability values from gh_{ij} according to the relative vector (dx,dy,dz) to neighboring data and combines them (equation 1) to update the conditional probability of the current facies.

Original：

Revision:

7.

Comment: Line 167: 'this' is ambiguous. Do you refer to Guo et al. 2024 or the work presented here?

Reply to the reviewer: Thanks for pointing this out. We clarified the sentence.

Original: '*Geophysical data can provide additional constraints to geostatistical simulations by linking lithological categories with physical properties (Guo et al., 2024).* ***In this study,*** *a stochastic resistivity–lithology relationship is established by deriving conditional probabilities from inverted resistivity models.*'

Revision: '*Geophysical data can provide additional constraints to geostatistical simulations by linking lithological categories with physical properties (Guo et al., 2024).* ***In the present study****, a stochastic resistivity–lithology relationship is established by deriving conditional probabilities from inverted resistivity models.*'

8.

Comment: It is not clear how P(A|C) is estimated nor how P(A|B,C) is integrated in the MCP framework (equation 1).

Reply to the reviewer: P(A|C) was derived from the inverted resistivity models through lithology–resistivity calibration. For the synthetic case, the entire training image (TI) was used to establish this relationship, whereas for the real-field case, borehole data were employed for calibration. During simulation, for a unsimulated node, the MCP algorithm first computes the conditional probability P(A|B), as according to equation 1, based on the bivariate probabilities derived from neighboring points. This probability is then immediately merged with the lithology–resistivity conditional probability P(A|C) using the permanence-of-ratios formulation (equation 5) to obtain P(A|B,C), which is subsequently used for random sampling to determine the lithofacies at that node.

Original:

Revision: The text was modified accordingly below equation 5.

9.

Comment: Line 231: what are the different variables composing the training image? (maybe insert a step between 4. And 5.).

Reply to the reviewer: We are not entirely certain that we understood this comment as intended.

Since the calculation of the joint probability has been clarified in the previous comment, we assume the question is related on how the training image was selected. For training image of the synthetic case described in Line 23, a manually synthetic three-layer lithological model was constructed on a 2D 80 × 50 grid. The training image (TI) used in the synthetic case corresponds to this simplified three-layer model, containing three categorical facies.

Original:

Revision:

10.

Comment: Figure 1 is confusing; there are two steps 6, crossing arrows, please reorganise it to make it clear or remove if the text description above is clear enough. Then later comes Figure 11, that looks totally different. It would be better to have a single workflow figure in section 2, and then give the specific of how the TI and conditional probabilities are estimated for the synthetic case and the real-case study.

Reply to the reviewer: A general workflow illustrating the constrained MCP working principle and the integration of geophysical data has been added at the end of Section 2. This figure provides an overview of how the MCP algorithm operates and how soft geophysical constraints are incorporated. Since the synthetic case and the real-field case have different objectives and slightly different workflow, we decided to keep a figure for both. For the synthetic case, the approach involves using the true lithological model to generate the synthetic conductivity distribution, applying a forward model to generate TEM sounding data, and performing a 1D inversion to obtain the conductivity model. For the real-field case, geophysical data already exist in this area, and we use lithological information to statistically link the lithology and resistivity data. We actually implemented this in a '3D' manner: multiple profiles were used as training images to derive bivariate probabilities, which were then merged into a general one containing more information, and finally applied to simulate multiple locations.

Original:

Revision: Provide a general workflow for the constrained MCP working principle at the end of Section 2.:

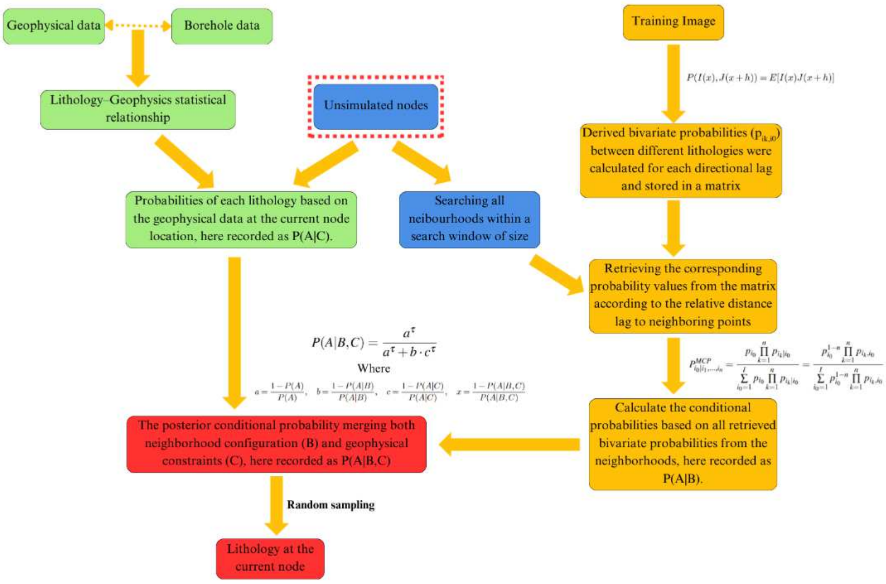

Also, the workflow plots of both the synthetic and field cases have been improved for clarity according to the comment.

Synthetic case:

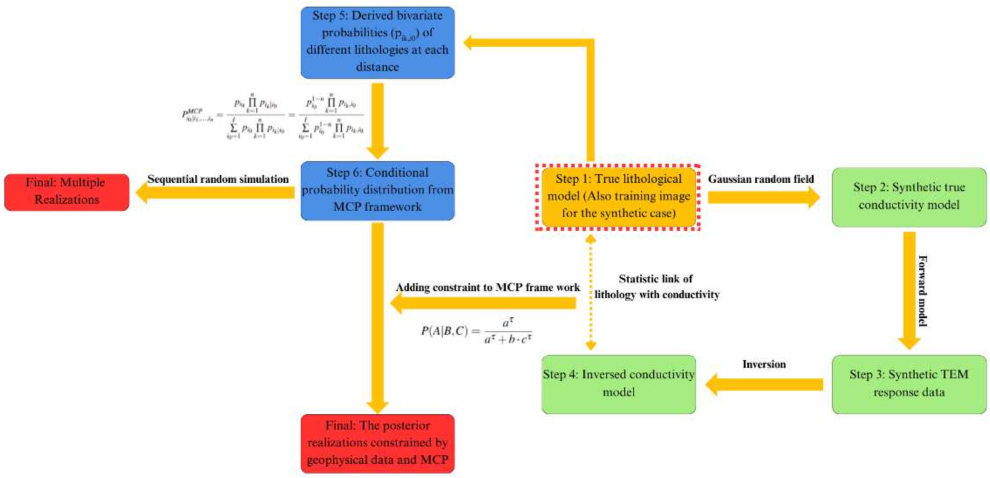

Real-field case:

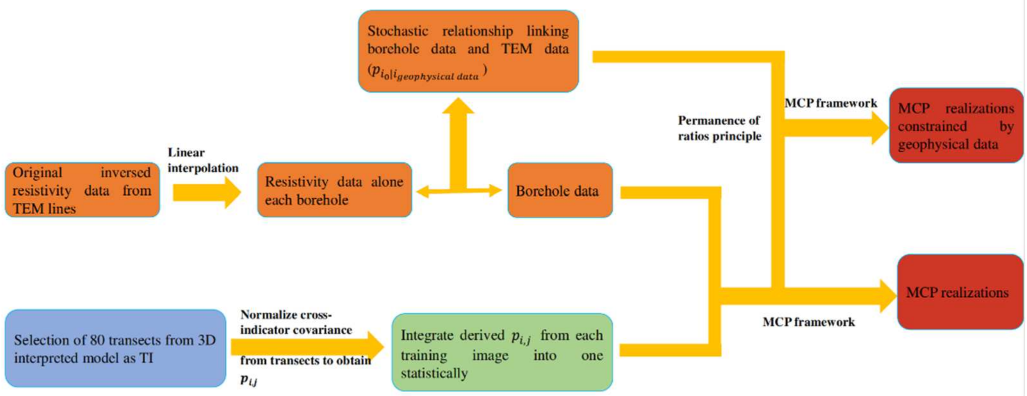

Results and discussion:

11.

Comment: Figure 9a: use the same colormap as in Figure 7.

Figure 9b: use a perceptually uniform colormap (e.g. https://doi.org/10.1038/s41467-020-19160-7 , https://www.fabiocrameri.ch/colourmaps/ , https://colorcet.com/)

Reply to the reviewer: Thanks very much for the helpful suggestion to improve the readability of the figures. The figures have been revised accordingly.

Original:

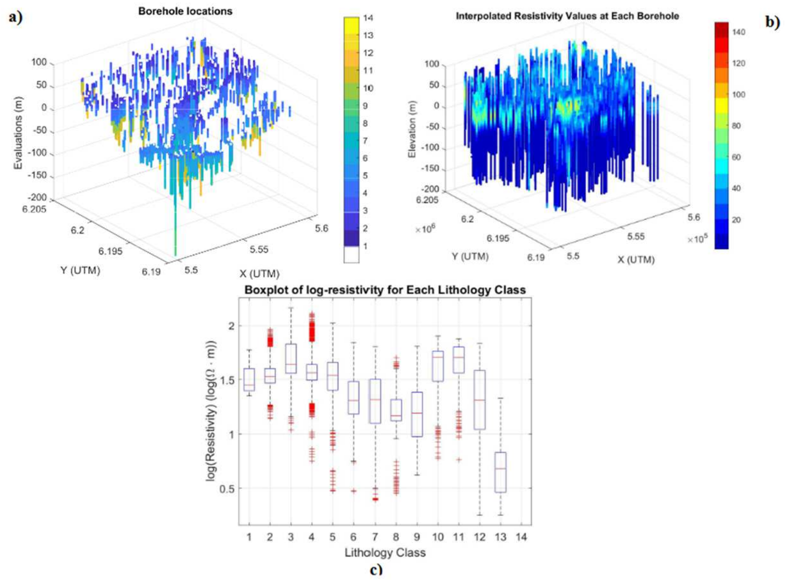

Figure 9. (**a**): Lithological information of each borehole. (**b**): Inverted resistivity values are interpolated along the borehole locations. (**c**): Inverted resistivity distribution with each lithology type based on interpolated resistivity values.

Revision:

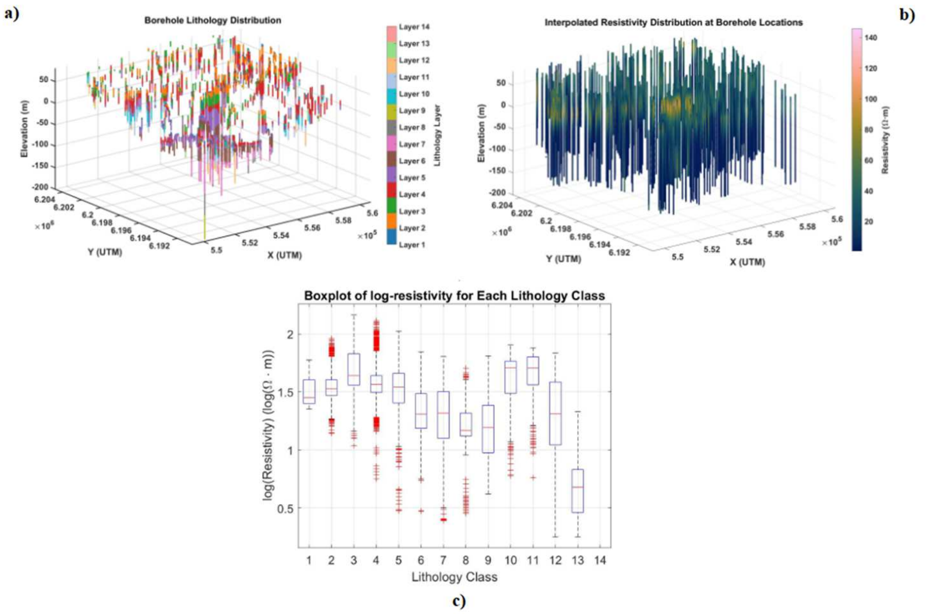

Figure 9. (**a**): Lithological information of each borehole. (**b**): Inverted resistivity values are interpolated along the borehole locations. (**c**): Inverted resistivity distribution with each lithology type based on interpolated resistivity values.

12.

Comment: Line 440-441, maybe add a reference to support the use of Shannon's entropy, e.g. one of the followings:

1. Lindsay, M. D., Aillères, L., Jessell, M. W., de Kemp, E. A., & Betts, P. G. (2012). Locating and quantifying geological uncertainty in three-dimensional models: Analysis of the Gippsland Basin, southeastern Australia. Tectonophysics, 546, 10-27.

2. Pirot, G., Joshi, R., Giraud, J., Lindsay, M. D., & Jessell, M. W. (2022). loopUI-0.1: indicators to support needs and practices in 3D geological modelling uncertainty quantification. Geoscientific Model Development, 15(12), 4689-4708.

Line 445: averaging lithological categorical values seems dangerous. It may convey false information. E.g. if lithologies 10 (aquifer) and 12 (aquifer) average to 11 (aquitard), that would not make sense. It would make more sense to have an aquitard probability volume and an aquifer probability volume.

Reply to the reviewer: The suggested reference is added to support the use of Shannon's entropy. We agree with the reasoning that if the interpretation is made in terms of properties of the layers, this could be misleading. However, in this case, we limit ourselves to the hydrostratigraphy itself. Since the layers are chronologically ordered, the average value is still meaningful in that sense. Nevertheless, both the expectation and entropy results demonstrate the same thing: the presence of the valley with geophysical constraints and reduced uncertainties. Therefore, it is sufficient to retain only the entropy results, and the average was removed.

Original：

For the uncertainty analysis of the real-field case, three types of plots were generated: expectation plots, entropy plots, and probability plots. However, the reviewer noted that producing expectation plots by averaging categorical classes can be misleading.

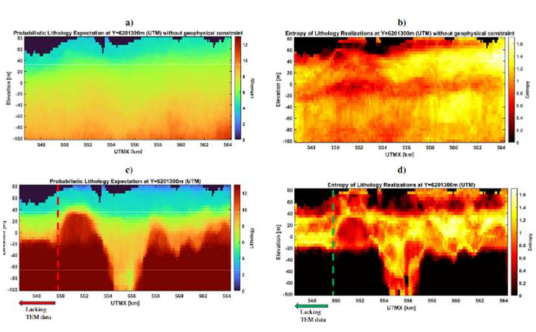

Figure 15. Uncertainty analysis at transect of $Y = 6201300$ (UTM), red dash lines represents the boundary of existence of TEM data: (a) (b): Entropy and expectation maps based on MCP realizations without geophysical constraint. (c) (d): Entropy and expectation maps based on MCP realizations adding geophysical constraint.

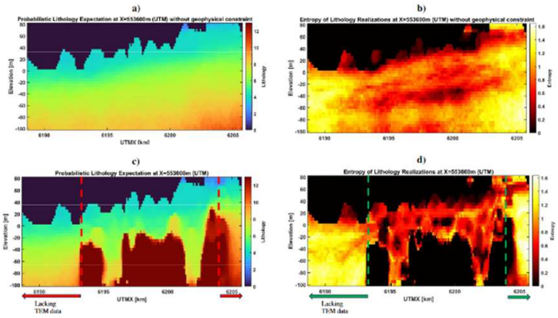

Figure 14. Uncertainty analysis at transect of $X = 553600$ (UTM), red dash lines represents the boundary of existence of TEM data: (a) (b): Entropy and expectation maps based on MCP realizations without geophysical constraint. (c) (d): Entropy and expectation maps based on MCP realizations adding geophysical constraint.

Revision: '*To better evaluate the uncertainty of added geophysical constraints in our MCP simulations, we computed entropy maps which measure the diversity of predicted lithology categories at each location based on the Shannon entropy (Pirot et al., 2022) across realizations, and probability maps for the two transects, under both constrained and unconstrained scenarios.*'

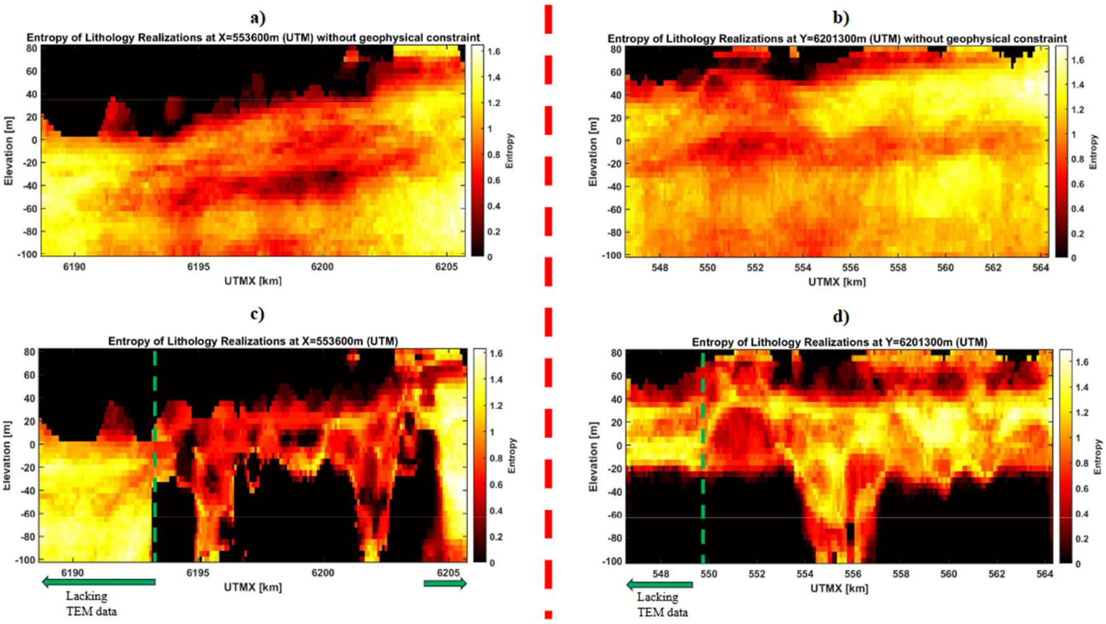

Figure 14. Uncertainty analysis based on entropy values, green dash lines represents the boundary of existence of TEM data: **(a) (c)**: Entropy maps based on MCP realizations along the transect at $X = 553600$ (UTM). **(a)** shows the case without geophysical constraints, while the lower panel shows the case with geophysical constraints. **(b) (d)**: Entropy maps based on MCP realizations along the transect at $Y = 6201300$ (UTM). The upper panel shows the case without geophysical constraints, while the lower panel shows the case with geophysical constraints.

13.

Comment: Line 504, is the interpreted geological model (Figure 7) used as reference in the sensitivity analysis? Please clarify.

Original:

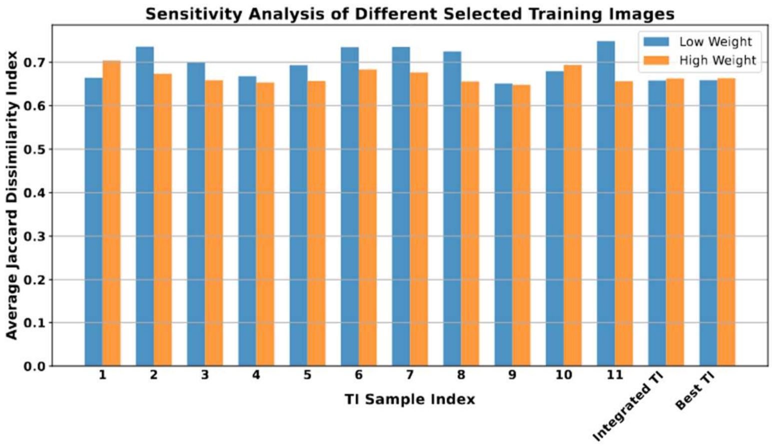

Figure 18. Sensitivity analysis of Training Image (TI) selection on lithological predictions using the MCP framework with geophysical constraints. The bar plot presents the average Jaccard dissimilarity index computed over 100 realizations for each of the 13 TI scenarios. These include 11 randomly selected TIs, one "Integrated TI" constructed from all 8 transects, and one "Best TI" using the current transect as the TI. Blue bars represent results under a low weight of geophysical constraint, while orange bars represent results under a high weight of geophysical constraint.

Revision: Reply to the reviewer: Yes. The sensitivity analysis used the interpreted geological model shown in the bottom right of Figure 7 (transect at Y=6201300 m) as the reference. For each TI selection option, we computed the Jaccard dissimilarity index between each of the 100 MCP realizations and this reference model, and then averaged the results to quantify the dissimilarity between the predicted and reference models for each TI choice.